Pertanika J. Sci. & Technol. 25 (S): 37 - 44 (2017)

SCIENCE & TECHNOLOGY

Journal homepage: http://www.pertanika.upm.edu.my/

Nonlinear Dynamic Inverse Controller Based in Field Oriented with SVPWM Current Control

Settar S. Keream[1,2]*, Ahmed N Abdalla[2] and Mohd Razali Bin Daud

[1]*College of Engineering, University of Anbar, Iraq*
[2]*University Malaysia Pahang, Malaysia*

ABSTRACT

A new Nonlinear Dynamic Inverse (NDI) method is proposed to minimise the ripple torque in an induction motor. This method is based on field oriented with space vector pulse width modulation (SVPWM). The nonlinear dynamic inverse controller cancelled a non-desirable response of the induction motor and enhancing the performance. This cancellation attempts by careful nonlinear algebraic equations. First, a mathematical model of induction motor and decoupling between two inputs have achieved. Then the desired new dynamic is derived from implementing the proposed nonlinear dynamic inverse controller (NDIC) technique that reserves some benefits such as fast torque control, minimum ripple torque, and fast speed response. Also, the proposed method significantly reduced the torque ripple which is the major concerns of the classical hysteresis-based in direct torque control (DTC) and feedback linearization control (FLC) scheme and have an effect on the stator current distortion. Finally, the simulation results with MATLAB/Simulink achieved for a 2-hp induction motor (IM) drive. The results are verification proved that the proposed (NDI-SVPWM) system achieves smaller torque ripple about 0.4% and faster torque response than the conventional SVM-based on proportional integral (PI-DTC) method.

Keywords: Dynamic inverse, induction motor, ripple torque

INTRODUCTION

Decreasing the ripple torque in the induction motor is a concern for many researchers because of its role in induction motor (IM) performance. Switching frequency varies with operating conditions and high torque ripple are two main problems of direct torque control (DTC) drives. As a result, induction motor (IM)'s which are robustness, low price, reliability and free maintenance, are used in industrial applications for a large scale.

ARTICLE INFO

Article history:
Received: 24 August 2016
Accepted: 03 Jun 2017

E-mail addresses:
settar_msc@yahoo.com;
pee13003@stude.ump.edu.my (Settar S. Keream),
ahmed@upm.edu.my (Ahmed N Abdalla),
mrazali@upm.edu.my (Mohd Razali Bin Daud)
*Corresponding Author

ISSN: 0128-7680

A direct torque control (DTC) with a simple flux regulation is presented in (Alsofyani and Idris 2016) for induction motor (IM) to improve torque and speed estimations at zero - and low -speed regions. In this system, in closed-loop speed control, the rotor speed feedback was estimated by extended Kalman filter based on real-time computation. However, a constant switching frequency controller (CSFC) was used due to the modest building of DTC-CSFC, small sampling time, hence significant control bandwidth was possible. Choi et al., (2016) presented a feedback which linearized direct torque control, and this control is with flux ripples for IPMSM drives and reduced torque. In this paper, the others succeed in reduction the torque and flux ripples to approximate (4-5) % with fast response to speed and torque varying conditions during the simulation process for uncertainties for some of the parameters. There is some difference between the simulation and experimental results. (Vafaie, Mirzaeian Dehkordi et al. 2016), proposed a new predictable DTC method via a voltage vector which has an optimal phase. This approach can improve the classical DTC's dynamic reaction as well as decrease torque ripples and flux ripples. By using space-vector modulation, which has five segments, the voltage vector that obtained the fixed frequency of switching was synthesized

This paper proposes a nonlinear dynamic inverse NDI technique to an induction motor. This method is used to minimize the ripple torque based on field-oriented current control with SVM. To apply the proposed NDI-SVPWM scheme, the decoupled dynamic model of an IM is first introduced by defining the two states (i.e., the stator flux and speed). The nonlinear dynamic inverse is applied to the nonlinear IM model to obtain an equivalent linearized model and then utilizing the linear control theory. The desired stator flux and rotor speed are adjusted with proportional integral derivative (PID) controller to get minimum allowed ripple torque with fast response. Consequently, the proposed method can significantly lessen the torque ripple which is the major weaknesses of the classical hysteresis-based DTC scheme. Simulation and investigations are carried out via MATLAB/Simulink of a 2-hp IM drive to confirm the performance of the proposed NDI-SVPWM scheme.Results indicate that the proposed NDI-SVPWM scheme realizes faster and low ripple torque of about 0.4%.Simulated results also confirm that the proposed method reduces the torque ripple effectively while improving the dynamic response of the traditional DTC and FLC methods, robust control under 100% parameter uncertainty.The proposed method helps to cancels undesired the behavior of induction motors caused by huge ripple torque and the instabilty of working under low speed and variable torque. After cancellation process by NDIC apply the desired input by a set of PID controller to get minimum allowed ripple torque with fast response.

Nonlinear Dynamic Inverse Controller

DI is a controller synthesis technique to cancel and replace deficient or undesirable dynamics with designer-specified desirable dynamics.

A tail-sitter vertical take-off and landing (VTOL) were used a hover flight attitude controller in the micro aerial vehicle (MAV) was presented by(Jin, Bifeng et al. 2015). Considering the aggravation affectability and nonlinear dynamics of the VTOL MAV, applying L1 versatile control hypothesis for augmenting the baseline dynamic inversion controller. The L1 versatile growth follows up on the evaluating, angular dynamics and compensating uncertainty in the

time-varying with fast adjustment rate and appropriate time-delay margin. The design of a self-scheduled current controller for doubly fed induction machines was presented by (Tien, Scherer et al. 2016) . The outline depended on the structure of straight parameter-shifting frameworks where the mechanical angular rate was thought to be a quantifiable time-changing parameter.

Current Control

Consider the field-oriented model of the induction motor (Boukas and Habetler 2004).

$$f(\dot{x}) = f(x) + B(x)u$$

$$f(x) = \begin{bmatrix} k\varphi_{rd} i_{sq} - \frac{f}{J}\Omega - \frac{T_l}{J} \\ -\alpha\varphi_{rd} + \alpha m_{sr} i_{sd} \\ p\Omega + \alpha m_{sr} \frac{i_{sq}}{\varphi_{rd}} \\ \alpha\beta\varphi_{rd} + \alpha m_{sr} \frac{i_{sq}^2}{\varphi_{rd}} + p\Omega i_{sq} - \epsilon i_{sd} \\ p\beta\Omega\varphi_{rd} - \alpha m_{sr} \frac{i_{sd} i_{sq}}{\varphi_{rd}} - p\Omega i_{sd} - \epsilon i_{sq} \end{bmatrix}, \quad B(x) = \begin{bmatrix} 0 & 0 \\ 0 & 0 \\ 0 & 0 \\ \frac{1}{\sigma L_s} & 0 \\ 0 & \frac{1}{\sigma L_s} \end{bmatrix}, u = \begin{bmatrix} v_{sd} \\ v_{sq} \end{bmatrix} \quad (1)$$

$$x = [\Omega, \varphi_{rd}, \theta_{rf}, i_{sd}, i_{sq}], \ \varphi_{rd} = \sqrt{\varphi_{r\alpha}^2 + \varphi_{r\beta}^2}, \theta_{rf} = \tan^{-1}\left(\frac{\varphi_{r\beta}}{\varphi_{r\alpha}}\right)$$

This model is field-oriented, and its frame (synchronous) is (d,q), where d stands for direct axis and q for the quadrate-axis. These are the axes of the rotor flux, which in this case is aligned with the direct axis, while the quadrate-axis component is zero.

Assume PID (proportional plus integral and derivative) current loops of the following form:

$$V_{sd} = k_{dp}(i_{sd}^* - i_{sd}) + k_{dI}\int(i_{sd}^* - i_{sd})\,dt + kdD\frac{d}{dt}(i_{sd}^* - i_{sd}) \quad (2)$$

$$V_{sq} = k_{qp}(i_{sq}^* - i_{sq}) + k_{qI}\int(i_{sq}^* - i_{sq})\,dt + kqD\frac{d}{dt}(i_{sd}^* - i_{sd}) \quad (3)$$

Where the symbol * denotes command inputs. For fast PID loops, we can assume the following:

$$i_{sd} = i_{sd}^* \quad (4)$$

$$i_{sq} = i_{sq}^*$$

A very realistic assumption, considering the performance of modem microprocessors and power electronics, which can achieve closed-loop control with a period of a few microseconds. Thus, the voltage-fed model (1) is reduced to the current-controlled field-oriented induction motor model, which is

$$\frac{d}{dt}\begin{bmatrix} \omega_r \\ \varphi_{rd} \\ \theta_{rf} \end{bmatrix} = \begin{bmatrix} \mu\varphi_{rd} i_{sq}^* - \frac{f}{J}\omega_r - \frac{T_L}{J} \\ -\alpha\varphi_{rd} + \alpha m_{sr} i_{sd}^* \\ p\omega_r + \alpha m_{sr} \frac{i_{sq}^*}{\varphi_{rd}} \end{bmatrix} \quad (5)$$

Speed Control in Stator-Oriented Model

This section deals with the application of the command matching control strategy to the stator-oriented induction motor model (Boukas and Habetler, 2004). The method is studied in depth for the current-fed field oriented control in the next section, which forms the main theoretic result of the current research. System (5) can be expressed in a more compact form as follows

$$\dot{x} = f(x) + B(x).u(t) \tag{6}$$

With output: y =C(x)

Where $x = [\Omega\ \varphi_{rd}\ \theta_{rd}]^T$ is the system state, u(t) is the input vectors, $C(x) = [\Omega\ \varphi_{rd}]^T$, and f(x), B(x) appropriate functions of the following form

$$f(x) = \begin{bmatrix} -\frac{f}{J}\Omega - \frac{T_L}{J} \\ -\alpha\varphi_{rd} \\ p\Omega \end{bmatrix}, \quad B(x) = \begin{bmatrix} 0 & k\varphi_{rd} \\ \alpha m_{sr} & 0 \\ 0 & \frac{\alpha m_{sr}}{\varphi_{rd}} \end{bmatrix} \tag{7}$$

The system (6) is divided into two subsystems: (7) which contain the disturbance (load torque), and (8).

$$\dot{\Omega} = k\varphi_{rd} i_{sq}^{*} - \frac{f}{J}\Omega - \frac{T_L}{J} \tag{8}$$

While (9) is formed from the last two equations of (4). It is expressed in compact form as

$$\dot{x}_1 = f_1(x) + B_1(x).u(t) \tag{9}$$

$y = C(x)$

Where $x_1 = [\varphi_{rd}\ \theta_{rd}]^T$ is the system state, u(t) is the input vectors, $C(x) = [\Omega\ \varphi_{rd}]^T$, and $f_1(x)$, $B_1(x)$ appropriate functions of the following form

$$f_1(x) = \begin{bmatrix} -\alpha\varphi_{rd} \\ p\Omega \end{bmatrix}, \quad B_1(x) = \begin{bmatrix} \alpha m_{sr} & 0 \\ 0 & \frac{\alpha m_{sr}}{\varphi_{rd}} \end{bmatrix} \tag{10}$$

The influence of the controlled subsystem (9) on (8) will be seen later when we form the closed-loop system from these two subsystems. Subsystem (10) is merely the last two equations of (7). At this point, the objective is to find an appropriate control input function u(t), to achieve input-output decoupling (i.e. y = u*) where u* is the external command vector ($\varphi^{*}_{rd}\ \Omega^{*}$ are the input commands for the rotor flux and the rotor mechanical speed, respectively).

$$u(t) = g_1^{-1}(x)[\dot{x}_1 - f_1(x) + u^{*} - c(x)] \tag{11}$$

Feeding (11) into (9) results in input-output decoupling

$$y(t) = u^* \tag{12}$$

The controller (11) is shown below regarding motor parameters to reveal its implementation simplicity:

$$I^*_{sd\_des} = \frac{1}{\alpha m_{sr}}\left[\left(\frac{d\varphi_{rd}}{dt} + \alpha\varphi_{rd}\right) + (\varphi^*_{rd} - \varphi_{rd})\right] \tag{13}$$

$$I^*_{sq\_des} = \frac{\varphi_{rd}}{\alpha m_{sr}}\left[\left(\frac{d\theta_{rf}}{dt} - p\Omega\right) + (\Omega^* - \Omega)\right]$$

Nonlinear Dynamic Inverse for Induction Motor

In this section, a more common approach (Settar S. Keream 2014) is presented for the dynamic inverse of the current fed motor model (1). The last two relations of the field-oriented motor model (1), which represent the dynamics of the stator windings, are:

$$\frac{d}{dt}\begin{bmatrix} i_{sd} \\ i_{sq} \end{bmatrix} = \begin{bmatrix} \alpha\beta\varphi_{rd} + \alpha m_{sr}\dfrac{i^2_{sq}}{\varphi_{rd}} + p\Omega i_{sq} - \epsilon i_{sd} \\ p\beta\Omega\varphi_{rd} - \alpha m_{sr}\dfrac{i_{sd}\, i_{sq}}{\varphi_{rd}} - p\Omega i_{sd} - \epsilon i_{sq} \end{bmatrix} + \frac{1}{\sigma L_s}\begin{bmatrix} v_{sd} \\ v_{sq} \end{bmatrix} \tag{14}$$

We need to find appropriate input $v=[v_{sd}, v_{sq}]^T$ to cancel the nonlinearities of the system (14). The controller is of the form:

$$v = \delta(x) + \zeta(x)u \tag{15}$$

Where x is the full state vector of the motor model (1) and $u=[u_{sd}, u_{sq}]^T$ external input vector. Consider the following choices for the functions of (15)

$$\delta(x) = \sigma L_s \begin{bmatrix} -\alpha\beta\varphi_{rd} - \alpha m_{sr}\dfrac{i^2_{sq}}{\varphi_{rd}} - p\Omega i_{sq} + \epsilon i_{sd} \\ -p\beta\Omega\varphi_{rd} + \alpha m_{sr}\dfrac{i_{sd} i_{sq}}{\varphi_{rd}} + p\Omega i_{sd} + \epsilon i_{sq} \end{bmatrix}, \zeta(x) = 1 \tag{16}$$

Applying the controller (15), (16) to system (14) results in:

$$\frac{d}{dt}\begin{bmatrix} i_{sd} \\ i_{sq} \end{bmatrix} = \begin{bmatrix} u_{sd} \\ u_{sq} \end{bmatrix} \tag{17}$$

Flux Estimator

The additional feature of the estimator, in this case, is the extraction of the flux magnitude and flux angle derivatives (φ_{rd} , θ_{rf}). The estimator equations have to be numerically solved during the control process (Leonhard 2001). For a fast control Digital Signal Processor (DSP)

this is a typical task. Numerical methods used for their solution are studied. The estimator relations follow

$$\frac{d}{dt}\begin{bmatrix}\hat{\varphi}_{rd}\\ \hat{\theta}_{rf}\end{bmatrix}=\begin{bmatrix}-\alpha\hat{\varphi}_{rd}+\alpha m_{sr} i_{sd}\\ p\omega_r+\alpha m_{sr}\dfrac{i_{sq}}{\hat{\varphi}_{rd}}\end{bmatrix} \tag{18}$$

Where the "hat" symbol indicates estimated quantities. The percentage ripple torque calculation is attempt by (Aghili, Buehler et al. 1998)

$$R\% = \frac{T_{max} - T_{min}}{T_{ss}} \times 100 \tag{19}$$

Where R% is the percentage ripple torque, T_{max} is the maximum torque, T_{min} is the minimum torque, T_{ss} is the steady state torque at a specific time.

Simulation Results and Discussion

Figure 1 explained the dynamic inverse controllers as in (15). Figure 2 illustrates the line output voltage of the inverter that provides AC to the induction motor that is controlled to the performance of the induction motor and achieved the desired response such as speed and torque. The fast response of rotor speed of the induction motor is shown in Figure3, at time 0.12 second the speed is stable at 40 Rad/Sec as desired. The torque response is showing in Figure4, the magnitude of input load torque is varied from (0.4-0.8) N.m to test the behaviour of the output torque response. Figure 5 is the zooming of the Figure 4 at a certain time to explain the shape of the ripple torque and calculated the ripple torque percentage (19) (which about 0.4%).

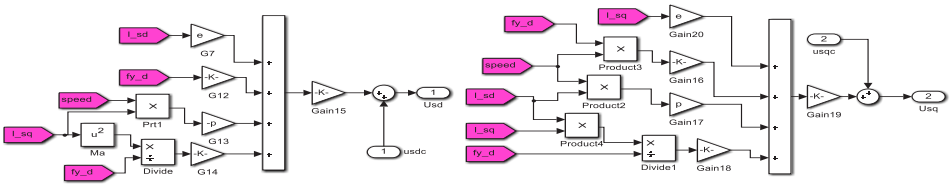

Figure 1. Block diagram of the dynamic inverse

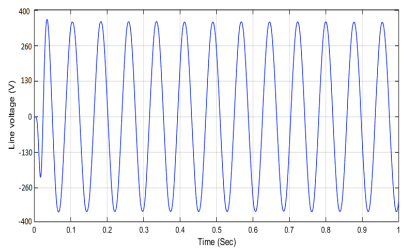

Figure 2. Output line voltage of the inverter

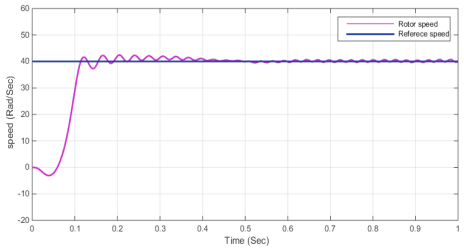

Figure 3. Rotor speed response with reference speed

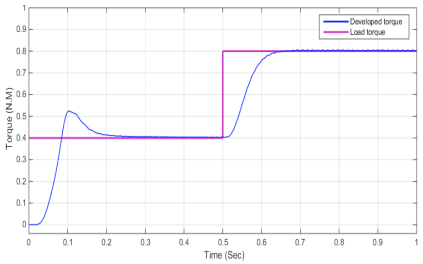

Figure 4. Developed torque response with variable load torque

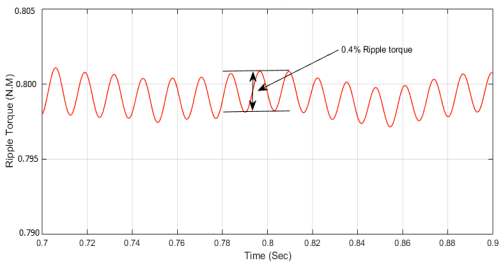

Figure 5. Ripple torque zooming for a given moment

Figure 6 and 7 illustrate the behavior of the rotor speed and torque under 100% uncertainty in stator resistance and rotor resistance and 20% uncertainty in mutual inductance.

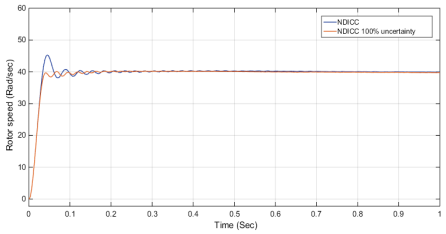

Figure 6. Rotor speed response with and without 100% uncertainty

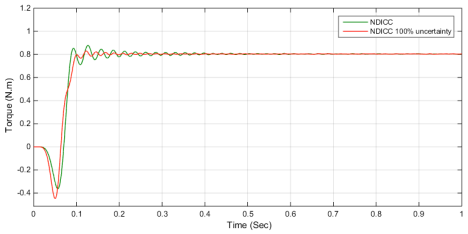

Figure 7. Torque response with and without 100% uncertainty

The three phase induction motor parameters are: Rated voltage 380 V, Power 2hp, Frequency 60Hz, Friction factor 0.0001 (N.m.s), Stator resistance and inductance (3.05Ω, 0.243H), Rotor resistance and inductance (2.12Ω, 0.306H), Mutual inductance 0.225H, Inertia 0.0005 (kg.m^2), Pole pairs 2.

CONCLUSION

This paper introduces a nonlinear dynamic inverse controller (NDI) that is applied on induction motor based in SVPWM to minimise the ripple torque. It shows the variation in torque magnitude (0.4-0.8) N.m does not have a harmful effect on the speed response stability through operation time. The results confirm that the proposed method is both robust and does not depend on induction motor parameters.

REFERENCES

Aghili, F., Buehler, M., & Hollerbach, J. M. (1998, October). Torque ripple minimization in direct-drive systems. In *IROS* (pp. 794-799).

Alsofyani, I. M., & Idris, N. R. N. (2016). Simple Flux Regulation for Improving State Estimation at Very Low and Zero Speed of a Speed Sensorless Direct Torque Control of an Induction Motor. *IEEE Transactions on Power Electronics, 31*(4), 3027-3035.

Boukas, T. K., & Habetler, T. G. (2004). High-performance induction motor speed control using exact feedback linearization with state and state derivative feedback. *IEEE Transactions on Power Electronics, 19*(4), 1022-1028.

Choi, Y. S., Choi, H. H., & Jung, J. W. (2016). Feedback linearization direct torque control with reduced torque and flux ripples for IPMSM drives. *IEEE Transactions on Power Electronics, 31*(5), 3728-3737.

Jin, W., Bifeng, S., Liguang, W., & Wei, T. (2015). L 1 Adaptive Dynamic Inversion Controller for an X-wing Tail-sitter MAV in Hover Flight. *Procedia Engineering, 99*, 969-974.

Leonhard, W. (2001). *Control of electrical drives*. Springer Science & Business Media.

Settar, S., Keream, A. N. A., Ghoni, R., Daud, M. R., & Al Mashhadany, Y. (2014). Robust Dynamic Inverse Controller For Spacecraft Mode. *International Journal of Scientific Research (IJSR), 3*(5), 113-117.

Tien, H. N., Scherer, C. W., Scherpen, J., & Muller, V. (2016). Linear Parameter Varying Control of Doubly Fed Induction Machines. *Industrial Electronics, IEEE Transactions on, 63*(1), 216-224.

Vafaie, M. H., Dehkordi, B. M., Moallem, P., & Kiyoumarsi, A. (2016). A New Predictive Direct Torque Control Method for Improving Both Steady-State and Transient-State Operations of the PMSM. *IEEE Transactions on Power Electronics, 31*(5), 3738-3753.

Zhang, B. Y., & Morton, B. (1998). Robustness analysis of dynamic inversion control laws applied to nonlinear aircraft pitch-axis models. *Nonlinear Analysis: Theory, Methods and Applications, 32*(4), 501-532.